

Isolation of the polysulfide complex $[(\text{UO}_2)(\text{S}_2)_3]^{4-}$ from the *in situ* formation and subsequent reaction of uranyl cations in molten alkali metal polysulfide salts

Anthony C. Sutorik and Mercuri G. Kanatzidis*

Department of Chemistry, Michigan State University, East Lansing, Michigan 48824, U.S.A.

(Received 5 February 1997; accepted 12 May 1997)

Abstract—The new uranyl polychalcogenide compounds $\text{Cs}_4(\text{UO}_2)(\text{S}_2)_3$ and $\text{Na}_4(\text{UO}_2)(\text{S}_2)_3 \cdot \text{Na}_2\text{S}_3$ were synthesized in molten polysulfide salts in the temperature range of 350–400°C and were characterized with single crystal X-ray crystallography. Both compounds contain the mononuclear anionic complex $[(\text{UO}_2)(\text{S}_2)_3]^{4-}$. The uranyl cation is coordinated to three chelating $(\text{S}_2)^{2-}$ species such that the midpoints of each disulfide define the equatorial positions of a trigonal bipyramidal coordination for U. © 1997 Elsevier Science Ltd

Keywords: polysulfide complex; flux synthesis; uranyl ion; molten salt; polychalcogenide complex.

The chemistry between metal cations and polychalcogenide ligands has been studied extensively over the years using a variety of solution based techniques [1]. This has led to a considerable amount of empirical knowledge concerning these complexes, although the various solution equilibria which polychalcogenides are prone to, based on their ability to undergo self-redox reactions, makes synthetic predictability difficult. In many systems the reaction of metals in molten polychalcogenide salts has been a valuable addendum to these studies. Generally, the new phases seen in molten salt reactions have tended to be solid state structures with extended covalent bonding, a sharp contrast to the discrete ionic complexes commonly resulting from solution [2]. For many elements, however, studying metal/ $(\text{Q}_x)^{2-}$ chemistry can be exceedingly difficult. Group 4 and 5 transition metals, lanthanides, and actinides can access high oxidation states and hence become very hard Lewis acids. These are especially oxophilic species which, when given a choice, would rather coordinate to oxygen containing (hard base) ligands rather than those with chalcogenide (soft base) binding sites. With molten A_2Q_x

fluxes, we can study the reaction of highly oxophilic metals with polychalcogenide ligands directly, without the need for any sort of polar solvent medium. Studies to date indicate that out of all the f-elements, U is most prone to give discrete molecular complexes under molten salt conditions. The triangulated dodecahedral 8-coordinate $[\text{U}(\text{Se}_2)_4]^{4-}$ complex forms from the reaction of U metal in molten K_2Se_x [3]. At first accidentally but then by design we discovered that U tends to form $(\text{UO}_2)^{2+}$ even in molten polychalcogenide salts. The uranyl cation is then coordinated by polysulfide ligands forming the discrete complexes found in the two new oxychalcogenide phases: $\text{Cs}_4(\text{UO}_2)(\text{S}_2)_3$ and $\text{Na}_4(\text{UO}_2)(\text{S}_2)_3 \cdot \text{Na}_2\text{S}_3$.

EXPERIMENTAL

Synthesis

Reagents. The following reagents were used as obtained: uranium metal, 60 mesh, Cerac, Milwaukee, WI; sulfur powder, sublimed, JT Baker Co., Phillipsburg, NJ; sodium metal, analytical reagent, Mallinckrodt Inc., Paris, KY; cesium metal, Johnson M. Matthey Co., Ward Hill, MA; copper metal-mesh,

* Author to whom correspondence should be addressed.

Fisher Scientific Co., methanol, anhydrous, analytical reagent grade, Mallinckrodt Inc., Paris, KY.

Cs₂S and Na₂S. Synthesis of these compounds was performed as described in ref [4].

Na₄(UO₂)(S₂)₃·Na₂S₃. In an N₂ filled glove box, 0.070 g (0.90 mmol) Na₂S, 0.060 g (0.25 mmol) U and 0.064 g (2.0 mmol) S were thoroughly mixed and loaded into a Pyrex tube. The tubes were removed from the box and evacuated on a Schlenk line to 3×10^{-5} torr and flame sealed. The reactants were heated at 400°C for 2 days and cooled to 200°C at 4°C/h, followed by quenching to 50°C. Excess polysulfide flux was removed, in the manner described previously, by washing with degassed DMF until the solvent remains clear, signaling complete polysulfide removal. The sample was decanted one final time and then dried under vacuum. The remaining product was a mixture of black powder and black, water-soluble, chunky crystals, which were subsequently found to be Na₄(UO₂)(S₂)₃·Na₂S₃ by single crystal X-ray diffraction.

Cs₄(UO₂)(S₂)₃. This phase was first observed as a member of an inhomogeneous product from the reaction of Cs₂S, Cu, U, and S. A mixture of 0.298 g (1.0 mmol) Cs₂S, 0.008 g (0.126 mmol) Cu, 0.030 g (0.126 mmol) U and 0.064 g (2.0 mmol) S were mixed and sealed into Pyrex tubes as described earlier. The reaction was heated in a computer-controlled furnace at 360°C for 2 days and cooled to 160°C at 4°C/h followed by quenching to 50°C. Excess flux was dissolved in the manner described earlier by using one portion of degassed methanol and several portions of degassed DMF. After drying under vacuum, the remaining material was a mixture of black, water-soluble needles and white powder. Single crystal analysis on the black needles subsequently revealed them to be Cs₄(UO₂)(S₂)₃.

Reproducible, high yield synthesis of Cs₄(UO₂)(S₂)₃ was achieved by the reaction of 0.223 g (0.78 mmol) Cs₂S, 0.030 g (0.126 mmol) U, 0.014 g (0.126 mmol) SeO₂, and 0.048 g (1.5 mmol) S. The reagents were thoroughly mixed in an N₂ filled glove box and loaded into a Pyrex tube. The tubes were removed from the box and evacuated on a Schlenk line to 3×10^{-3} torr and flame sealed. The reactants were heated at 360°C for 2 days and cooled to 160°C at 4°C/hr, followed by quenching to 50°C. Excess polysulfide flux was removed by dissolving it in successive portions of degassed methanol in the manner previously described. The remaining material is black needles with a very small amount of red-brown, apparently amorphous, powder. The identity of the black needles was confirmed by comparing its powder X-ray diffraction pattern against one calculated using the coordinates obtained from the X-ray single crystal analysis (see Table 1). Fourier transform Raman spectroscopy was used as an independent confirmation of the identity and purity of the product. The phase is insoluble in methanol and DMF but is rapidly dissolved, and presumably decomposed, in distilled

Table 1. Calculated and observed X-ray powder diffraction pattern for Cs₄(UO₂)(S₂)₃ (Cu radiation)

<i>h</i>	<i>k</i>	<i>l</i>	<i>d</i> _{calc} /(Å)	<i>d</i> _{obs} /(Å)	^{1/4} I _{max} obs (%)
0	2	0	7.07	7.06	83.25
2	2	0	3.990	3.977	26.86
1	3	-1	3.982		
1	2	-1	3.970		
0	4	0	3.533	3.529	52.22
2	2	1	3.524		
1	3	1	3.513		
3	-2	1	3.504		
3	0	1	3.453		
3	1	0	3.445	3.448	8.52
2	-4	0	3.354		
3	1	-1	3.340	3.346	29.18
3	-3	0	3.328		
2	3	0	3.270	3.276	20.48
0	4	-2	3.150	3.164	33.25
4	-1	0	2.894	2.898	17.31
3	-3	2	2.869		
2	-5	0	2.792	2.790	51.17
2	4	0	2.730	2.733	27.62
1	-3	-3	2.485		
3	-1	3	2.483	2.480	30.77
3	-1	-3	2.474		
0	1	-4	2.469		
3	1	-3	2.469		
0	6	0	2.355	2.352	100.00
4	-4	-2	2.142	2.142	21.82
1	5	2	2.139		
4	4	-2	1.9419	1.9331	20.48
6	-1	-2	1.7996	1.7998	10.31
0	8	0	1.7666	1.7639	78.01
3	7	-1	1.6561	1.6499	31.59

water. Also the compound will visibly degrade upon overnight exposure to air.

Physical measurements

The instrumentation and experimental setup for powder X-ray diffraction, infrared spectroscopy, and UV-vis/near IR spectroscopy (diffuse reflectance mode) have been described elsewhere [5].

Raman spectroscopy

Raman spectra were obtained on a Biorad FT Raman instrument with a 1064 nm Nd:YAG laser source. Samples used were neat powders loaded into capillary tubes for analysis.

Single crystal X-ray diffraction

Single crystals of compounds in this section were treated as air-sensitive materials. The crystals were coated in mineral oil to protect them from the atmo-

Table 2. Crystallographic data for $\text{Cs}_4(\text{UO}_2)(\text{S}_2)_3$ and $\text{Na}_4(\text{UO}_2)(\text{S}_2)_3 \cdot \text{Na}_2\text{S}_3$

Formula	$\text{Cs}_4(\text{UO}_2)(\text{S}_2)_3$	$\text{Na}_4(\text{UO}_2)(\text{S}_2)_3 \cdot \text{Na}_2\text{S}_3$
a (Å)	11.579(5)	7.180(3)
b (Å)	14.751(9)	7.286(3)
c (Å)	9.879(6)	28.83(1)
α (°)	100.43(6)	
β (°)	90.23(4)	93.17(7)
γ (°)	102.79(4)	
V (Å ³)	1617(2)	1506(2)
Space group	$P\bar{1}$	$P2_1/c$
Z	2	4
F.W. (g/mol)	994.01	696.51
d_{calc} (g/cm ³)	4.084	3.496
μ (cm ⁻¹)	7.8	18.1
Crystal dimensions (mm ³)	0.02 × 0.10 × 1.00	0.20 × 0.20 × 0.40
Radiation	Mo-K α	Mo-K α
2θ max. (°)	50.2	50
data collection temp. (°C)	23	-70
No. data collected	6007	3000
No. unique data	5697	2541
No. $F_o^2 > 3\sigma(F_o^2)$	3707	1695
No. of variables	235	163
R/R_w , %	5.5/7.1	5.8/7.3
Final Dif. map max. peak, e ⁻ /Å ³	2.76	2.81

$$^a R = \Sigma(|F_o| - |F_c|) / \Sigma|F_o|; R_w = \{\Sigma w(|F_o| - |F_c|)^2 / \Sigma w|F_o|^2\}^{1/2}.$$

sphere during mounting for single crystal diffraction studies. Each crystal was loaded into a thin walled glass capillary of diameter appropriate to the size of crystal. The capillary was carefully snapped to an appropriate length, and the crystal was held in place by drawing a fast hardening glue into the glass fiber with capillary action. The capillary was then mounted into an aluminum stub, held in place with paraffin wax, and inserted into a goniometer head for analysis.

Intensity data were collected using a Rigaku AFC6S four-circle automated diffractometer equipped with a graphite crystal monochromator. An ω - 2θ scan mode was used. The stability of the crystal was monitored with three standard reflections whose intensities were checked every 150 reflections, and unless noted, no crystal decay was detected. An empirical absorption correction based on ψ scans was applied to all data during initial stages of refinement. An empirical DIFABS correction [6] was applied after full isotropic refinement, after which full anisotropic refinement was performed. The structures were solved by direct methods using SHELXS-86 software [7a] (for all compounds), and full matrix least squares refinement was performed using the TEXSAN software package [7b]. Crystallographic data for the compounds are given in Table 2. Fractional atomic coordinates for the two phases are given in the Supplementary Material.

RESULTS AND DISCUSSION

Single crystals of $\text{Na}_4(\text{UO}_2)(\text{S}_2)_3 \cdot \text{Na}_2\text{S}_3$ were first observed from the reaction of U metal in a Na_2S_x flux. The source of oxygen contamination was determined

to be aged Na_2S as reactions using a fresh batch did not yield the phase. Several attempts at rational synthesis were made, none of which ever lead to $\text{Na}_4(\text{UO}_2)(\text{S}_2)_3 \cdot \text{Na}_2\text{S}_3$.

Although salts of various uranyl cations are commercially available, it was feared that the presence of too many extra species in the A_2Q_x flux would impair reaction homogeneity. Hence to rationally synthesize $\text{Cs}_4(\text{UO}_2)(\text{S}_2)_3$, the *in situ* formation of $(\text{UO}_2)^{2+}$ was performed by reacting stoichiometric amounts of U metal and SeO_2 in excess Cs_2S_x flux. Selenium dioxide was chosen as an oxygen source because (1) as a solid it is convenient to manipulate in these closed tube reactions; (2) it should readily decompose to liberate two O^{2-} anions as the highly oxidized Se^{4+} cations partially oxidize the surrounding polychalcogenide environment and (3) the Se would be in such small amounts, relative to the sulfides of the flux, that its incorporation into a resulting product would be unlikely.

$\text{Cs}_4(\text{UO}_2)(\text{S}_2)_3$ and $\text{Na}_4(\text{UO}_2)(\text{S}_2)_3 \cdot \text{Na}_2\text{S}_3$

Structure. $\text{Cs}_4(\text{UO}_2)(\text{S}_2)_3$ is composed of discrete anions separated by intervening Cs^+ cations. Figure 1 shows a view of one of these species: a $[(\text{UO}_2)(\text{S}_2)_3]^{4-}$ anion. The uranyl cation is coordinated to three $(\text{S}_2)^{2-}$ species such that it the midpoint of each disulfide is treated as a hypothetical atom, then the coordination about the U^{6+} would be trigonal bipyramidal. Each disulfide is in an η^2 chelation mode with all the sulfur atoms nearly coplanar with the central U atom which

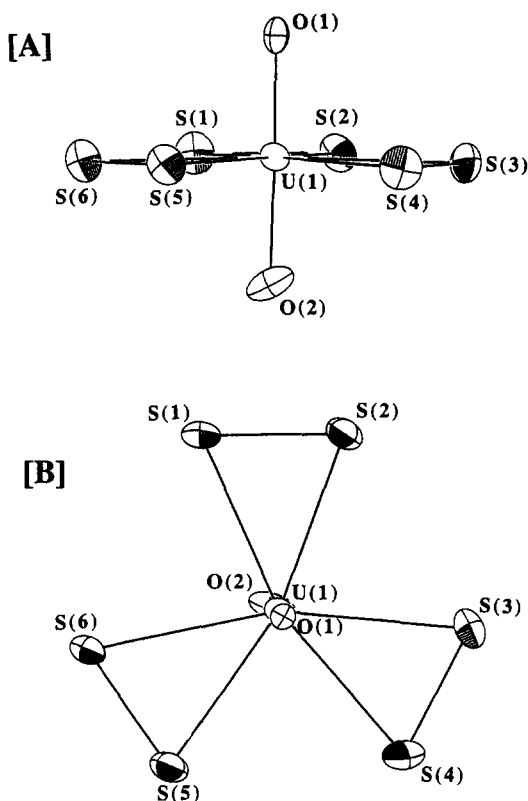


Fig. 1. Two views of the $[(\text{UO}_2)(\text{S}_2)_3]^{4-}$ anion in the Cs salt: (A) parallel and (B) perpendicular to the equatorial plane.

is 0.004 Å above the calculated least squares plane while the S atoms range from 0.030 to 0.054 Å below it. Meanwhile, the oxygen atoms of the uranyl are almost perfectly perpendicular to this equatorial plane of disulfides; the S—U—O angles in this compound only range from 88.6(6) to 91.7(7)°. Because of the strong double bonds between U and O in the uranyl, coordination about the equatorial plane of the cation is a characteristic feature. The uranyl has been known to accommodate anywhere from four to six atoms in these equatorial sites. Several structural analogs to the $[(\text{UO}_2)(\text{S}_2)_3]^{4-}$ anion exist such as the long known peroxide form, $\text{Na}_4[(\text{UO}_2)(\text{O}_2)_3] \cdot 9\text{H}_2\text{O}$ [8], and $\text{Na}[(\text{UO}_2)(\text{O}_2\text{CCH}_3)_3]$ [9], $\text{Rb}[(\text{UO}_2)(\text{NO}_3)_3]$ [10], and $[\text{Me}_4\text{N}][(\text{UO}_2)(\text{S}_2\text{CN}(\text{C}_2\text{H}_5)_2)_3]$ [11] in which the bulk of the three chelating groups forces the coordinating atoms to lie alternatively above and below the uranyl equatorial plane.

There are two crystallographically distinct $[(\text{UO}_2)(\text{S}_2)_3]^{4-}$ anions in each asymmetric unit of the structure, and Table 3 provides a summary of the bond distances and angles of both. Both anions are suspended inside octahedral shaped pockets defined by Cs^+ ions and anchored *via* O—Cs interactions. The O=U=O axis is perpendicular to two triangular faces of the Cs_6 octahedron with an average Cs—O of 3.12 Å (see Fig. 2). The range of U—S bonds is 2.772–2.837 Å, and comparable values are seen for eight

coordinate U in $\text{Cu}_2\text{U}_6\text{S}_{13}$ (2.702–2.939 Å) [12]. The U—O bonds range from 1.79(2) to 1.86(2) Å while in $\text{Na}_4[(\text{UO}_2)(\text{O}_2)_3] \cdot 9\text{H}_2\text{O}$ the corresponding uranyl distances were 1.814(2) and 1.909(2) Å [8]. The bond distances in the disulfides are particularly invariant at either 2.08(1) or 2.09(1) Å, which are comparable to the values for the S—S bonds in α - and β - KCuS_4 (2.056–2.089 Å) [13].

Crystallizing as the Na+ salt does little to alter the environment around the U atom. Bond distances for $\text{Na}_4[(\text{UO}_2)(\text{S}_2)_3] \cdot \text{Na}_2\text{S}_3$ are given in Table 4, and they are all comparable to what has been seen in the Cs^+ analog. In fact in this lattice as well as the $[(\text{UO}_2)(\text{S}_2)_3]^{4-}$ anion sits inside a very similar Na^+ octahedral pocket with an average Na—O distance of 2.43 Å. This compound is a double salt as the cocrystallization of Na_2S_3 signifies. That the simple salt $\text{Na}_4[(\text{UO}_2)(\text{S}_2)_3]$ does not form suggests that the smaller Na ion may not be capable of a stable lattice arrangement. The presence of Na_2S_3 may play the role of a lattice filler and attests to the strong tendency in this system to form the discrete $[(\text{UO}_2)(\text{S}_2)_3]^{4-}$ anion. On its own, this uranyl complex seems to be resisting the drive towards an extended isomeric structure with bridging S—S bonds. The geometry of the $[\text{S}_3]^{2-}$ anion in this compound (see Table 4) is similar to those observed in other cases [14].

The anions in $\text{Cs}_4(\text{UO}_2)(\text{S}_2)_3$ pack in a surprisingly ordered fashion. The packing view given in Fig. 3 shows how the cations have naturally aggregated into one-dimensional pseudo-chains parallel to the *c* axis. There seems to be a segregation of atoms into layers possibly driven by $\text{Cs}^+—\text{Cs}^+$ repulsions, where each layer contains both anions and cations. The sulfur atoms from anion to anion maintain planarity with each other, but do not interact directly as the shortest inter-anion S—S distance is only 4.34 Å. This lack of interaction suggests merely a packing effect which is probably driven by the large Cs^+ cations. Their volume is such that the anions can remain well separated and so can arrange themselves more efficiently in order to minimize the void space. Despite the lack of interaction, seeing these well stacked anions suggests that some sort of extended covalent anionic structure may be possible in this system with the appropriate conditions. Such conditions may be achieved through a drastic reduction of the cation volume by means of substitution with smaller alkali atoms or with divalent cations or the application of pressure. The cocrystallization of the trisulfide fragment in the Na^+ salt demonstrates that, on its own, the discrete uranyl ions seem to have appreciable stability, and so an alternative approach would be to introduce a species which would covalently bridge the uranyl centers, as was done in the synthesis of $\text{Na}_4\text{Cu}_2(\text{UO}_2)\text{S}_4$, [15].

Spectroscopy. The Raman spectrum of $\text{Cs}_4(\text{UO}_2)(\text{S}_2)_3$ shows peaks at 701, 500, and 220 cm^{-1} . Uranyl cations have a characteristic vibration for the U—O double bond in the range 880–950 cm^{-1} [16], although bands as low as 730 cm^{-1} were observed in

Table 3. Selected bond distances (Å) and angles (°) for $Cs_4(UO_2)(S_2)_3$ (standard deviations in parentheses)

U(1)—S(1)	2.837(9)	U(2)—S(7)	2.793(8)
U(1)—S(2)	2.77(6)	U(2)—S(8)	2.816(8)
U(1)—S(3)	2.788(9)	U(2)—S(9)	2.823(9)
U(1)—S(4)	2.79(1)	U(2)—S(10)	2.804(8)
U(1)—S(5)	2.790(8)	U(2)—S(11)	2.772(9)
U(1)—S(6)	2.831(9)	U(2)—S(12)	2.781(9)
U(1)—O(1)	1.79(2)	U(2)—O(3)	1.82(2)
U(1)—O(2)	1.86(2)	U(2)—O(4)	1.80(2)
S(1)—S(2)	2.08(1)	S(7)—S(8)	2.08(1)
S(3)—S(4)	2.08(1)	S(9)—S(10)	2.09(1)
S(5)—S(6)	2.09(1)	S(11)—S(12)	2.08(1)
S(1)—U(1)—S(2)	43.4(3)	S(7)—U(2)—S(8)	43.5(3)
S(1)—U(1)—S(3)	119.1(3)	S(7)—U(2)—S(9)	120.5(3)
S(1)—U(1)—S(4)	162.8(3)	S(7)—U(2)—S(10)	164.0(3)
S(1)—U(1)—S(5)	121.6(3)	S(7)—U(2)—S(11)	120.1(3)
S(1)—U(1)—S(6)	78.0(2)	S(7)—U(2)—S(12)	76.0(3)
S(1)—U(1)—O(1)	91.5(6)	S(7)—U(2)—O(3)	88.3(6)
S(1)—U(1)—O(2)	88.3(7)	S(7)—U(2)—O(4)	90.3(6)
S(2)—U(1)—S(3)	75.8(3)	S(8)—U(2)—S(9)	77.0(2)
S(2)—U(1)—O(1)	91.2(6)	S(8)—U(2)—O(3)	88.6(6)
S(2)—U(1)—O(2)	89.6(6)	S(8)—U(2)—O(4)	89.8(6)
S(3)—U(1)—S(4)	43.8(3)	S(9)—U(2)—S(10)	43.6(3)
S(3)—U(1)—O(1)	91.3(7)	S(9)—U(2)—O(3)	89.5(6)
S(3)—U(1)—O(2)	90.0(8)	S(9)—U(2)—O(4)	90.5(7)
S(4)—U(1)—S(5)	75.4(3)	S(10)—U(2)—S(11)	75.8(3)
S(4)—U(1)—O(1)	91.0(7)	S(10)—U(2)—O(3)	89.5(6)
S(4)—U(1)—O(2)	89.6(8)	S(10)—U(2)—O(4)	91.6(6)
S(5)—U(1)—S(6)	43.6(3)	S(11)—U(2)—S(12)	44.0(2)
S(5)—U(1)—O(1)	90.2(6)	S(11)—U(2)—O(3)	89.7(6)
S(5)—U(1)—O(2)	88.7(6)	S(11)—U(2)—O(4)	91.7(7)
S(6)—U(1)—O(1)	90.9(6)	S(12)—U(2)—O(3)	89.1(7)
S(6)—U(1)—O(2)	87.7(7)	S(12)—U(2)—O(4)	91.4(7)
O(1)—U(1)—O(2)	178.6(9)	O(3)—U(2)—O(4)	178.4(8)

Table 4. Selected bond distances (Å) and angles (°) for $Na_4(UO_2)(S_2)_3 \cdot Na_2S_3$ (standard deviations in parentheses)

U(1)—S(1)	2.741(6)	S(1)—S(2)	2.084(9)
U(1)—S(2)	2.765(6)	S(3)—S(4)	2.085(9)
U(1)—S(3)	2.777(6)	S(5)—S(6)	2.094(8)
U(1)—S(4)	2.793(6)	S(7)—S(8)	2.075(9)
U(1)—S(5)	2.739(6)	S(8)—S(9)	2.08(1)
U(1)—S(6)	2.784(6)		
U(1)—O(1)	1.84(2)	U(1)—O(2)	1.86(2)
S(1)—U(1)—S(2)	44.5(2)	S(3)—U(1)—O(1)	91.0(5)
S(1)—U(1)—S(3)	119.5(2)	S(3)—U(1)—O(2)	89.9(5)
S(1)—U(1)—S(4)	163.4(2)	S(4)—U(1)—S(5)	75.6(2)
S(1)—U(1)—S(5)	120.8(2)	S(4)—U(1)—O(1)	91.3(5)
S(1)—U(1)—S(6)	76.3(2)	S(4)—U(1)—O(2)	89.1(5)
S(1)—U(1)—O(1)	91.2(5)	S(5)—U(1)—S(6)	44.5(2)
S(1)—U(1)—O(2)	88.7(5)	S(5)—U(1)—O(1)	90.9(5)
S(2)—U(1)—S(3)	75.1(2)	S(5)—U(1)—O(2)	88.3(5)
S(2)—U(1)—O(1)	92.0(5)	S(6)—U(1)—O(1)	89.8(5)
S(2)—U(1)—O(2)	88.6(5)	S(6)—U(1)—O(2)	89.3(5)
S(3)—U(1)—S(4)	44.0(2)	O(1)—U(1)—O(2)	179.1(7)
		S(7)—S(8)—S(9)	102.1(4)

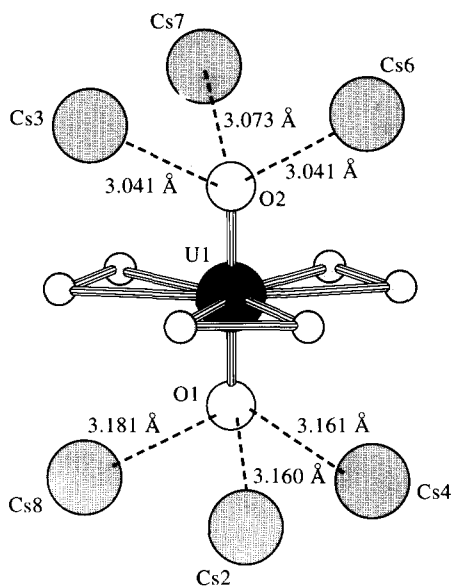


Fig. 2. The octahedral pocket of Cs ions which surrounds the $[(\text{UO}_2)(\text{S}_2)_3]^{4-}$ anion.

$\text{Na}_4[\text{UO}_2(\text{O}_2)_3] \cdot 9\text{H}_2\text{O}$ [8]. The proximity of the 701 cm^{-1} peak in the Raman spectrum to this frequency range indicates it is from the uranyl. The peak at 500 cm^{-1} corresponds to S-S stretches observed in known polysulfide compounds [17], and the low energy peak of 220 cm^{-1} is assigned to U-S vibrations.

The solid state diffuse reflectance optical absorbance spectrum of $\text{Cs}_4(\text{UO}_2)(\text{S}_2)_3$ is shown in Fig. 4. Two peaks are observed: one at 1.7 eV and a second at 2.3 eV. Their origin probably lies in charge transfer from a mainly sulfur p orbital to a primarily uranyl $6d/5f$ orbital. Because the phase contains discrete anions, the orbital overlap between anions is very limited. Thus, a discrete electronic transitions are seen

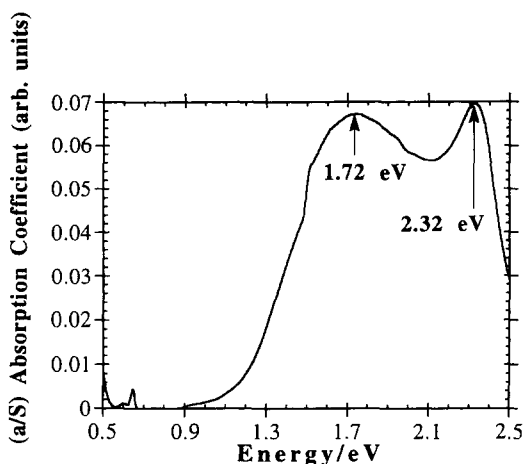


Fig. 4. The solid state diffuse reflectance spectra of $\text{Cs}_4(\text{UO}_2)(\text{S}_2)_3$ plotted as absorption coefficient (a/S) vs energy (eV).

in $\text{Cs}_4(\text{UO}_2)(\text{S}_2)_3$, rather than the sharp absorption edges associated with band gaps.

CONCLUSION

The addition of SeO_2 seems to be a good way to introduce oxygen into a molten salt reaction system involving oxophilic metals. Not only does the synthesis of $[(\text{UO}_2)(\text{S}_2)_3]^{4-}$ call for a further examination of $(\text{UO}_2)^{2+}$ chemistry in other molten A_2Q_x salts, but it also gives strong indication that other oxymetal cations could also be used as stable building blocks in A_2Q_x fluxes. This is particularly intriguing in the case of asymmetric cations such as $(\text{TiO})^{2+}$, $(\text{VO})^{2+}$, $(\text{MoO})^{3+}$, and $(\text{WO})^{3+}$, whose incorporation into solid state lattices could potentially lead to materials with acentric space groups.

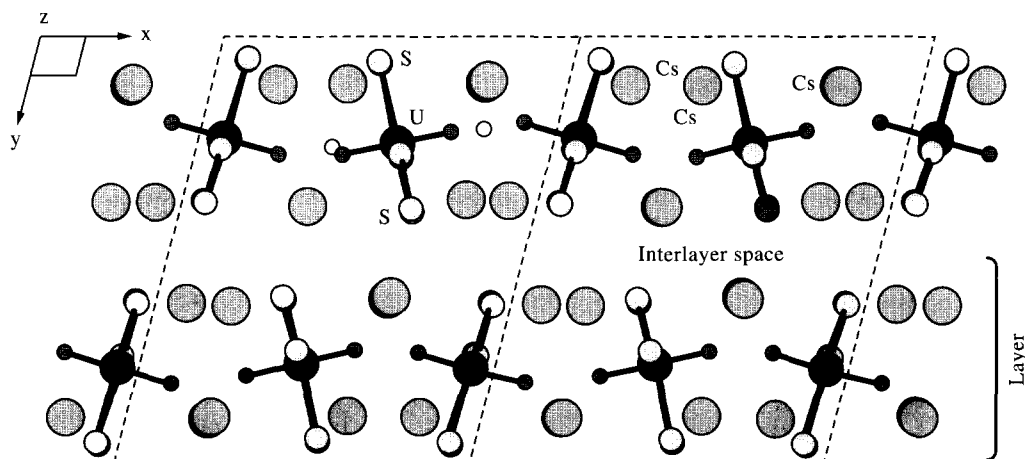


Fig. 3. The unit cell of $\text{Cs}_4(\text{UO}_2)(\text{S}_2)_3$ as seen parallel to the b -axis.

Acknowledgements—Financial support from the National Science Foundation DMR-9527347 is gratefully acknowledged. This work made use of the SEM and TEM facilities of the Center for Electron Optics at Michigan State University.

Supplementary material—Fractional atomic coordinates of $\text{Cs}_4(\text{UO}_2)(\text{S}_2)_3$ and $\text{Na}_4(\text{UO}_2)(\text{S}_2)_3 \cdot \text{Na}_2\text{S}_3$.

REFERENCES

1. (a) Flomer, W. A. and Kolis, J. W., *J. Am. Chem. Soc.*, 1988, **110**, 3682; (b) Kanatzidis, M. G., and Huang, S.-P., *Coord. Chem. Rev.*, 1994, **130**, 509; (c) Kolis, J. W., *Coord. Chem. Rev.*, 1990, **105**, 195.
2. Kanatzidis, M. G. and Sutorik, A. C., *Prog. Inorg. Chem.*, 1995, **43**, 151–265, and refs therein.
3. Sutorik, A. and Kanatzidis, M. G., *J. Am. Chem. Soc.*, 1991, **113**, 7754.
4. Sutorik, A. C., Albritton-Thomas, J., Kannewurf, C. R. and Kanatzidis, M. G., *J. Am. Chem. Soc.*, 1994, **116**, 7706.
5. Sutorik, A. C., Albritton-Thomas, J., Hogan, T., Kannewurf, C. R. and Kanatzidis, M. G., *Chem. Mat.*, 1996, **8**, 751.
6. Walker, N. and Stuart, D., *Acta Cryst.*, 1983, **A39**, 158.
7. (a) Sheldrick, G. M., in *Crystallographic Computing 3*, Sheldrick, G. M., Kruger, C., Doddard, R., Eds., p. 175–189. Oxford University Press: Oxford (1985); (b) Gilmore G. J., *Appl. Cryst.*, 1984, **17**, 42.
8. Alcock, N. W., *J. Chem. Soc. (A)*, 1968, 1588.
9. Zachariassen, W. H. and Plettinger, H. A., *Acta Cryst.*, 1959, **12**, 526.
10. Barclay, G. A., Sabine, T. M. and Taylor, J. C., *Acta Cryst.*, 1965, **19**, 205.
11. Bowman, K. and Dori, Z., *J. Chem. Soc., Chem. Commun.*, 1968, 636.
12. Noel, H. and Potel, M., *J. Less-Common Met.*, 1985, **113**, 11.
13. Park, Y. and Kanatzidis, M. G., *J. Am. Chem. Soc.*, 1989, **111**, 3767.
14. (a) Boettcher, P., *Z. Anorg. Allg. Chem.*, 1977, **432**, 167; (b) Boettcher, P., *Z. Anorg. Allg. Chem.*, 1980, **461**, 13.
15. Sutorik, A. and Kanatzidis, M. G., *J. Am. Chem. Soc.*, in press.
16. Perry, D. L., Zalkin, A., Ruben, H. and Templeton, D. H., *Inorg. Chem.*, 1982, **21**, 237.
17. Park, Y. and Kanatzidis, M. G., *J. Am. Chem. Soc.*, 1989, **111**, 3767.